

# Electronic Structure Analysis of the Nonlinear Optical Materials 4-Nitropyridine *N*-Oxide (NPO) and 3-Methyl-4-nitropyridine *N*-Oxide (POM)

Rainer Glaser\* and Grace Shiahuy Chen†

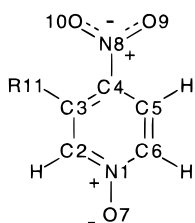
Department of Chemistry, University of Missouri—Columbia, Columbia, Missouri 65211

Received August 12, 1996. Revised Manuscript Received October 30, 1996<sup>®</sup>

The molecules 4-nitropyridine *N*-oxide (NPO) and 3-methyl-4-nitropyridine *N*-oxide (POM) and the models nitromethane and *N*-methylnitron were studied with ab initio electronic structure theory at the RHF level and with the inclusion of electron correlation using perturbation and density functional theories. At the highest level, MP2(full)/6-311G\*\*//MP2(full)/6-31G\*, the dipole moments  $\mu(\text{NPO}) = 0.97$  and  $\mu(\text{POM}) = 0.89$  D were obtained. Methyl substitution leads to only a small reduction of  $\Delta\mu < 0.1$  D and the computed dipole moments are in excellent agreement with recent experimental data. The dipole vector of NPO points away from the nitro group (−pole) toward the NO group (+pole) and the dipole vector in POM is rotated such as to point toward the Me-substituted half. The electric quadrupole moments of NPO and POM indicate quadrupolarity {− + −} along all axes and the  $|Q_{zz}|$  values are particularly large. Natural Population analysis reveals the common electronic motif for NPO and POM consisting in an electron-deficient hydrocarbon midsection embedded between electron-rich functional groups. The dipole direction in the pyridine *N*-oxides thus does not reflect contributions by the quinoid resonance form (electron density shifts from the NO to the NO<sub>2</sub> group) to the ground-state electronic structure. The directions of the molecular dipole moments of the pyridine *N*-oxides are the simple result of vector addition of the two inward pointing dipoles that are associated with the functional groups and caused by electronegativity differences. In contrast to X-ray electron density studies, the electronic consequences of H/Me replacement are found to be localized. Approximate “molecular dipole moments” based on point charge models (PCM) are compared to the correct dipole moments. The analysis of the PCM-derived dipole moments shows that a discussion of solid-state effects on the molecular dipole moments of NPO and POM must be postponed until the true dipole moments in the crystal have been more rigorously established.

## Introduction

Zyss et al. demonstrated that molecular nonlinear properties<sup>1</sup> can be realized with materials with vanishing dipole moments.<sup>2</sup> Pyridine *N*-oxide (PO) allowed for substitution in its 4-position such as to ensure near dipole cancellation, and the parent system, 4-nitropyridine *N*-oxide (NPO), and its 3-methyl derivative, 3-meth-



NPO, R = H

POM, R = Me

yl-4-nitropyridine *N*-oxide (POM), were indeed found to be efficient SHG materials in solution. However, NPO crystallizes in centrosymmetric space groups (poly-

morphs  $P2_1/c$  and  $Pnma$ ) and it is therefore NLO-inactive in the solid state. Sigelle et al.<sup>3</sup> showed that POM retains the NLO properties while crystallizing in the noncentrosymmetric space group  $P2_12_12_1$ . The X-ray structure of POM had been determined earlier by Shiro et al.,<sup>4</sup> and a recent study by Munn and Hurst<sup>5</sup> shows that the dipole sum in POM crystals nearly vanishes. Subsequently, the electrooptic (EO) coefficients of POM crystals were measured by Sigelle and Hierle,<sup>6</sup> and Zyss et al. also determined the acoustic and acoustooptic properties<sup>7</sup> and studied the second harmonic and sum-frequency generation in POM.<sup>8</sup> POM can be grown in pure and large single crystals,<sup>9</sup> and it has become an important and commercially used organic NLO material.

The structure, dipole moment, and vibrational properties of NPO have been well characterized. In 1957, Katritzky et al.<sup>10</sup> reported the dipole moments of series of 4-substituted pyridines and pyridine *N*-oxides and

† Presented at the 212th National Meeting of the American Chemical Society, Orlando, FL, August 1996.

\* Corresponding author. E-mail: chemrg@showme.missouri.edu.

® Abstract published in *Advance ACS Abstracts*, December 15, 1996.

(1) *Molecular Nonlinear Optics, Materials, Physics, and Devices*; Zyss, J., Ed.; Academic Press: New York, 1994.

(2) (a) Zyss, J.; Chemla, D. S.; Nicoud, J. F. *J. Chem. Phys.* **1981**, *74*, 4800. (b) Zyss, J. *J. Non-Cryst. Solids* **1982**, *47*, 211.

(3) Sigelle, M.; Zyss, J.; Hierle, R. *J. Non-Cryst. Solids* **1982**, *47*, 287.

(4) Shiro, M.; Yamakura, M.; Kubota, T. *Acta Crystallogr.* **1977**, *B33*, 1549.

(5) Munn, R. W.; Hurst, M. *Chem. Phys.* **1990**, *147*, 35.

(6) Sigelle, M.; Hierle, R. *J. Appl. Phys.* **1981**, *52*, 4199.

(7) Sapriel, J.; Hierle, R.; Zyss, J.; Boissier, M. *Appl. Phys. Lett.* **1989**, *55*, 2594.

(8) Dou, S. X.; Josse, D.; Hierle, R.; Zyss, J. *J. Opt. Soc. Am. B* **1992**, *9*, 687.

(9) Hierle, R.; Badan, J.; Zyss, J. *J. Cryst. Growth* **1984**, *69*, 545.

**Table 1. Experimental and Theoretical Dipole Moments for NPO and POM<sup>a</sup>**

method	NPO $ \mu $	POM				ref
		$\mu_x$	$\mu_z$	$\alpha$ (deg)	$ \mu $	
oscillator, benzene sol.	0.69					10
oscillator, benzene sol.	0.88					11
X-ray $\kappa$ refinement	0.4					16
X-ray $\kappa$ refinement I					1.6(1.3)	17
X-ray $\kappa$ refinement II					1.6(1.3)	17
X-ray $\kappa$ refinement III					3.56(1.4)	17
PPP/X-ray structure	0.15					11
CNDO/2, part. opt.	0.62					13
MNDO, part. opt.	0.93					13
CNDO					0.48	18
RHF/MIDI-basis I	1.53					19
RHF/MIDI-basis II	0.49					19
POM1, RHF/MIDI-II		0.45	-0.18		0.48	19
POM2, RHF/MIDI-II		0.20	0.08		0.22	19
IC oscillator	0.83				0.69	21
RHF/6-31G*	0.27	-0.80	-0.05	93.5	0.80	
MP2(full)/6-31G*	0.95	-0.67	0.58	49.2	0.88	
Becke3LYP/6-31G*	1.25	-0.79	0.89	41.6	1.18	
RHF/6-311G**	0.24	-0.87	-0.09	96.1	0.87	
MP2(full)/6-311G**	0.97	-0.67	0.59	48.7	0.89	
Becke3LYP/6-311G**	1.25	-0.83	0.88	43.2	1.21	

<sup>a</sup> Dipole moments in debye (D). 1 D =  $3.336 \times 10^{-30}$  C m. The dipole components given were normed to match the reported total dipole moment.

dipole moments of  $4.24$  and  $0.69 \pm 0.02$  D were found for PO and NPO, respectively. Yamakawa et al.<sup>11</sup> carried out semiempirical studies of the electronic spectrum on NPO.<sup>12</sup> The  $\pi$ - $\pi^*$  CT band at 346 nm was assigned to charge transfer from the NO centered HOMO to the NO<sub>2</sub> group centered LUMO. A dipole moment of 0.15 D was calculated with the Pariser-Parr-Pople (PPP) approximation and based on the solid-state structure of NPO (Table 1). The dipole moment  $\mu(\text{NPO}) = 0.88$  D was measured in benzene solution at 25 °C. As part of a study of the protonation of pyridine *N*-oxides, Churzynski et al.<sup>13</sup> reported dipole moments for NPO of 0.62 and 0.93 D based on semiempirical CNDO/2 and MNDO calculations using partially optimized structures. The X-ray structure of NPO was determined at 30 K by Wang et al.<sup>14</sup> and this study was complemented by a neutron diffraction study by Coppens and Lehmann<sup>15</sup> at the same low temperature. The data allowed for the study of deformation densities and X-N maps. Coppens and co-workers developed a method to assign net atomic charges and (approximate) molecular dipole moments from spherical atom X-ray refinements.<sup>16</sup> NPO was among the crystals analyzed in this way and the  $\kappa$  refinement led to a dipole moment of 0.4 D. Thus, all methods agree that the dipole moment of NPO is small (0.15–0.88 D) and the solution data indicate  $0.8 \pm 0.1$  D.

In contrast to NPO, the measurement of the dipole moment of POM posed a long-standing problem due to

POM's low solubility. Early estimates of  $\mu(\text{POM})$  came from solid-state and gas-phase studies. In 1988, Baert et al.<sup>17</sup> reported a structural and vibrational analysis. The solid-state structure of POM was studied at low temperature using neutron and high-order refinement X-ray diffraction techniques. The conformation of the methyl group was found to have the in-plane methyl-H pointing away from the proximate NO<sub>2</sub> group. An approximate molecular dipole moment was determined by refinement of atom populations (adjustable population  $P$ ) and the radial dependencies (adjustable parameter  $\kappa$ ) of spherical atom valence shells. The equation  $\rho_{\text{atom}}(r) = \rho_{\text{core}}(r) + P_{\text{valence}}(r) \cdot \rho_{\text{valence}}(\kappa r)$  was evaluated in several ways that dealt with the H atoms in different ways. Refinement I fixed the positional and anisotropic thermal parameters at the neutron values, refinement II employed TLS+ $\Omega$  model thermal parameters, and refinement III allowed for H position variations. Baert et al.<sup>17</sup> favored the dipole moment  $\mu(\text{POM}) = 3.56$  D derived from refinement III and pointed out that "there is an important discrepancy concerning the value of  $\mu_D$ " between POM and the value for NPO determined by Coppens et al.<sup>16</sup> with the same technique. This surprising conclusion did not remain unchallenged. Several estimates of the dipole moment of POM are provided by theory. Docherty et al.<sup>18</sup> computed a dipole moment of 0.48 D for POM using their version of CNDO/S semiempirical theory. In 1992, Berthier et al.<sup>19</sup> reported SCF calculations of the dipole moments and polarizabilities of PO, NPO, and POM. Two variations of the MIDI basis set were used with the larger one containing split p-AOs but no polarization functions. The molecule was considered in conformations POM1 (in-plane methyl-H points away from NO<sub>2</sub> group) and POM2 (in-plane methyl-H points to a NO<sub>2</sub> group) and structures were adapted from the literature (NPO geometry with standard methyl group). Small dipole moments of 0.22 (POM2) and 0.48 D (POM1) were found, and it was concluded that the dipole moment of 3.5 D determined earlier by crystallographic methods was overestimated. This conclusion was corroborated by the fact that the values computed with basis II for PO (4.80 D) and NPO (0.47 D) agreed well with experimental data for PO (4.24 D) and NPO (0.69–0.4 D). In the theoretical SCF/MIDI study by Berthier et al.<sup>19</sup> the directions of the dipole moments varied greatly with the theoretical level, and  $\alpha$  angles greater than 90° were found for the conformation of POM considered in the present study (POM1). In their 1994 study of the electronic excitation of NPO and POM, Briffaut-Le Guinier et al.<sup>20</sup> computed the ground state and the lowest excited state of NPO at the HF level using an unpolarized split-valence basis set, an unpolarized triply split valence basis set II, and a polarized basis set III which is otherwise identical with basis set II. Structures were optimized with basis set I and refined (NO only) using basis set II. Electron

(10) Katritzky, A. R.; Randall, E. W.; Sutton, L. E. *J. Chem. Soc.* **1957**, 1769.

(11) Yamakawa, M.; Kubota, T.; Ezumi, K.; Mizumo, Y. *Spectrochim. Acta* **1974**, *30*, 2103.

(12) For a study of the UV spectrum of the pyridine *N*-oxide and the changes of the molecular dipole moment associated with excitation, see: Seibold, K.; Wagniere, G.; Labhart, H. *Helv. Chim. Acta* **1969**, *52*, 789.

(13) Chmurzynski, L.; Liwo, A.; Tempczyk, A. *Z. Naturforsch.* **1989**, *44b*, 1263.

(14) Wang, Y.; Blessing, R. H.; Ross, F. K.; Coppens, P. *Acta Crystallogr.* **1976**, *B32*, 572.

(15) Coppens, P.; Lehmann, M. S. *Acta Crystallogr.* **1976**, *B32*, 1777.

(16) Coppens, P.; Guru-Row, T. N.; Leung, P.; Stevens, E. D.; Becker, P. J.; Yang, Y. W. *Acta Crystallogr.* **1979**, *A35*, 63.

(17) Baert, F.; Schweiss, P.; Heger, G.; More, M. *J. Mol. Struct.* **1988**, *178*, 29.

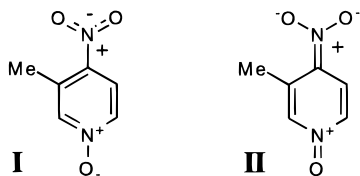
(18) (a) Docherty, V. J.; Pugh, D.; Morley, J. O. *J. Chem. Soc., Faraday Trans. 2* **1985**, *81*, 1179. (b) This computed value would suggest an even lower experimental dipole moment because of the correlation  $\mu_{\text{expt}} = 0.75\mu_{\text{CNDO}}$ . (c) Note that Munn and Hurst used this greatly underestimated dipole moment in their study of the screened dipole energy in POM.

(19) Berthier, G.; Defranceschi, M.; Lazzaretti, P.; Tsoucaris, G.; Zanasi, R. *J. Mol. Struct. (THEOCHEM)* **1992**, *254*, 205.

(20) Briffaut-Le Guinier, F.; Plaza, P.; Dao, N. Q.; Bénard, M. *Chem. Phys.* **1994**, *182*, 313.

deformation maps obtained using the largest basis set were discussed but no dipole moments were reported. The issue of the apparent differences between the electronic structures of NPO and POM has now been settled in that new gas phase and solution data on POM consistently indicate only a small deviation between the dipole moments of NPO and POM. The dipole moment of POM in solution was measured for the first time by Chen et al. and the accuracy of the method was ascertained by comparison to NPO.<sup>21</sup> Dipole moments of  $0.83 \pm 0.04$  and  $0.69 \pm 0.05$  D were determined for NPO and POM in millimolar benzene solution. These solution data are in excellent agreement with the values of  $\mu(\text{NPO}) = 0.97$  and  $\mu(\text{POM}) = 0.89$  D computed at the MP2/6-311G\*\*//MP2/6-31G\* level of perturbation theory.

The vibrational spectra of NPO and POM have been well characterized. Joyeux et al. studied the vibrational force field of NPO using semiempirical MNDO theory with both the MNDO and the AM1 parameters.<sup>22</sup> After Baert et al.<sup>17</sup> reported the IR and Raman spectra of POM with partial assignments, Plaza et al.<sup>23</sup> reported a complete vibrational analysis of POM and discussed the charge-transfer phenomenon observed in solution. The IR and Raman spectra of POM were recorded in the solid state and in saturated solution ( $\text{CS}_2$ ,  $\text{CCl}_4$ , MeOH) and assigned in analogy to NPO.



It was found that  $\nu_s(\text{N-O})$  decreases in proton donor solvents suggesting an decreased involvement of the quinoid resonance form in protic solvents. Most recently, Briffaut-Le Guinier et al.<sup>24</sup> determined a generalized valence force field of POM starting from the force constants of NPO. The perturbation by the methyl group was found to be rather small, and five frequencies of POM were reassigned in the process of the normal-coordinate analysis.

This brief review demonstrates the significant attention that has been dedicated to NPO and POM because of their interesting optical properties. In particular, the discussion highlights that both the measurements of accurate dipole moments as well as their reproduction with theoretical methods have only recently become possible. These advances are the requisites to the discussions of the electronic structures of NPO and POM which are the subject of the present paper. Improvements in both hardware and algorithms now permit electronic structure analyses at levels of ab initio theory that greatly exceed previously achievable theoretical levels. Specifically, we have completely optimized the structures of NPO and POM not only using Hartree–

Fock theory but also with the inclusion of electron correlation effects and in conjunction with polarized split-valence basis sets. The molecular dipole moments are employed to judge the quality of the theoretical methods against experimental data. The electronic structures of NPO and POM are characterized by their molecular quadrupole moments and atomic point charge models are described. Dipole moments derived from point charge models were determined, and they are compared critically to the correctly calculated molecular dipole moment.

## Computational Methods

Calculations<sup>25</sup> were performed with Gaussian94<sup>26</sup> and earlier versions on a cluster of IBM RS-6000 and Silicon Graphics Power Challenge L and Indigo systems. NPO and POM were fully optimized in  $C_{2v}$  and  $C_s$  symmetry, respectively, using restricted Hartree–Fock (RHF) theory, second-order Møller–Plesset theory with inclusion of all electrons in the correlation treatments [MP2-(full)], and density functional theory<sup>27</sup> using the hybrid method Becke3LYP.<sup>28</sup> The optimizations employed the 6-31G\* basis set, and six Cartesian d-type basis functions were employed. The first and second energy derivatives were computed analytically at RHF/6-31G\* and Becke3LYP/6-31G\* levels to confirm that stationary structures were indeed obtained. Electrical properties often are sensitive to the flexibility of the basis set, and we therefore also performed single-point calculations at the above levels using the more fully polarized valence triple- $\zeta$  quality basis set 6-311G\*\*. Sets of five d-type polarization functions were used in conjunction with the larger basis set. Properties computed with the 6-311G\*\* basis set are documented in Tables 2–5, while the respective data determined with the 6-31G\* basis set are contained in the Supporting Information.

## Results and Discussion

The optimized structures of NPO and POM are displayed in Figure 1, and comparison is made to the neutron diffraction studies of NPO by Coppens and Lehman<sup>15</sup> and of POM by Baert et al.<sup>17</sup> The RHF-derived data suffer from previously recognized deficiencies even when polarized basis sets are employed. The agreement is better at the correlated levels. Electron correlation lengthens the NO bonds and the NO bonds of the  $\text{NO}_2$  group are improved. Even in the MP2 optimized structures, the nitroxide N–O bonds still

(21) Chen, G. S.; Liu, C. S.; Glaser, R.; Kauffman, J. F. *Chem. Commun.* **1996**, 1719.

(22) (a) Joyeux, M.; Dao, N. Q. *Spectrochim. Acta* **1988**, *44A*, 1447. (b) Joyeux, M.; Martins Costa, M. T. C.; Rinaldi, D.; Dao, N. Q. *Spectrochim. Acta* **1989**, *45A*, 967.

(23) Plaza, P.; Le Guinier, F.; Joyeux, M.; Dao, N. Q.; Zyss, J.; Hierle, R. J. *Mol. Struct.* **1991**, *247*, 363.

(24) Briffaut-Le Guinier, F.; Dao, N. Q.; Jouan, M.; Plaza, P. *Spectrochim. Acta* **1994**, *50A*, 2091.

(25) Hehre, W. J.; Radom, L.; Schleyer, P. v. R.; Pople, J. A. *Ab Initio Molecular Orbital Theory*; John Wiley & Sons: New York, 1986.

(26) (26) *Gaussian94*, Revision C.3; Frisch, M. J.; Trucks, G. W.; Schlegel, H. B.; Gill, P. M. W.; Johnson, B. G.; Robb, M. A.; Cheeseman, J. R.; Keith, T.; Petersson, G. A.; Montgomery, J. A.; Raghavachari, K.; Al-Laham, M. A.; Zakrzewski, V. G.; Ortiz, J. V.; Foresman, J. B.; Cioslowski, J.; Stefanov, B. B.; Nanayakkara, A.; Challacombe, M.; Peng, C. Y.; Ayala, P. Y.; Chen, W.; Wong, M. W.; Andres, J. L.; Replogle, E. S.; Gomperts, R.; Martin, R. L.; Fox, D. J.; Binkley, J. S.; Defrees, D. J.; Baker, J.; Stewart, J. J. P.; Head-Gordon, M.; Gonzalez, C.; and Pople, J. A. Gaussian, Inc.: Pittsburgh, PA, 1995.

(27) (a) March, N. H. *Electron Density Theory of Atoms and Molecules*; Academic Press, Inc.: San Diego, CA, 1992. (b) Labanowski, J. K.; Andzelm, J. W., Eds. *Density Functional Methods in Chemistry*; Springer-Verlag: New York, 1991. (c) Parr, R. G.; Yang, W. *Functional Theory of Atoms and Molecules*; Oxford University Press: New York, 1989.

(28) (a) Becke, A. D. *Phys. Rev. A* **1986**, *33*, 2786. (b) Becke, A. D. *J. Chem. Phys.* **1988**, *88*, 2547. (c) Lee, C.; Yang, W.; Parr, R. G. *Phys. Rev. B* **1988**, *37*, 785.

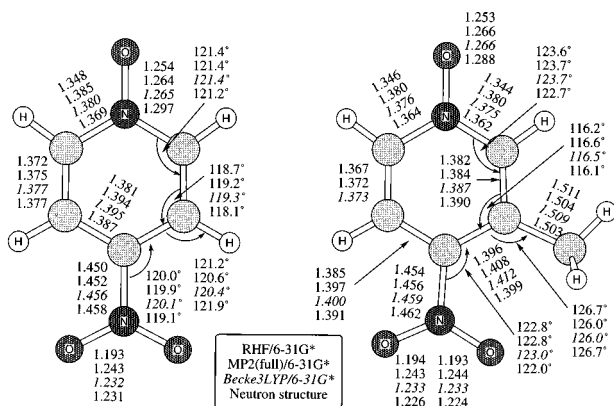
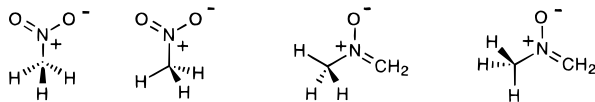


**Figure 1.** Optimized structures of NPO ( $C_{2v}$ ) and POM ( $C_s$ ) at the levels RHF/6-31G\*, MP2/6-31G\*, and Becke3LYP/6-31G\* and comparison to the structures determined by neutron diffraction.

deviate by up to 0.03 Å from the best neutron data. Some of these differences might have to do with packing effects but it is also likely that still higher theoretical levels will further alter the computed structures.

**Dipole Moments of NPO and POM and of Model Compounds.** Computed dipole moments are included in Table 1, and they appear nearly independent of the basis set; the dipole moments determined with the 6-31G\* and 6-311G\*\* basis sets differ by no more than 0.07 D. RHF theory is well-known to overestimate bond polarities and the inclusion of electron correlation usually reduces the dipole moment of dipolar species. In the present case of the quadrupolar 4-nitropyridine *N*-oxides the same is true for the dipole moments of both functional groups. While the combined effect of these two functional groups is small, correlation effects on the local electron density distributions are indeed substantial. We considered the model systems nitromethane,  $\text{CH}_3\text{NO}_2$ , and *N*-methylformaldimine *N*-oxide,  $\text{H}_2\text{C}=\text{N}(\text{O})\text{CH}_3$ , in  $C_s$  symmetry.



Nitromethane has been the subject of numerous theoretical and experimental studies.<sup>29</sup> These studies show that the methyl rotation is essentially free and that the *staggered* structure is only a few calories per mole more stable than the *eclipsed* structure.<sup>30</sup> Both methyl conformations were considered for the imine *N*-oxide, the nitrone,<sup>31</sup> and there is a preference for the conformation in which the in-plane methyl-H is *anti* with

respect to the NO bond. Nitrones are isomers of nitroso compounds and oximes,<sup>32</sup> and they have been the subject of several theoretical studies. The nitrone was studied at the RHF/6-31G\* level by Boyd and Boyd in their studies of spin traps.<sup>33</sup> Other studies discussed reactions of nitrones with various 1,3-dipolarophiles<sup>34</sup> and the oxaziridine ring-opening reaction.<sup>35</sup> We are particularly interested in the dipole moments of nitrones,<sup>36</sup> and they are listed in Table 2. As with NPO and POM, the dipole moments of the model systems vary but little with the choice of the basis set, but they do show rather substantial changes in magnitude depending on the theoretical level. The RHF dipole moments can be overestimated by as much as 1 D. At the best level, we find dipole moments of  $\mu(\text{CH}_3\text{NO}_2) = 3.35$  and  $\mu(\text{nitrone}) = 3.45$  D. The dipole moment of  $3.46 \pm 0.02$  D was measured for free  $\text{CH}_3\text{NO}_2$  by microwave spectroscopy,<sup>30a</sup> and this value is in excellent agreement with our best estimate. The dipole moment of nitromethane in pure liquid also has been determined via the Onsager equation and the resulting dipole moment of 3.44 D closely agrees with the gas-phase value.<sup>37</sup> It appears that neither the dipole moment of the parent nitrone nor the dipole moments of any small alkyl derivatives are known. Experimental values exist only for series of  $\alpha$ -phenyl *N*-methyl nitrones<sup>38</sup> and the  $\alpha$ -phenyl *N*-methyl nitrone itself has a dipole moment of 3.55 D.<sup>38b</sup> For the parent nitrone, dipole moments of 4.03 and 3.86 D were reported at the CNDO/2 and INDO levels,<sup>39</sup> and these seem overestimated in light of our results.

NPO was aligned such that its  $C_2$  axis coincided with the  $z$  axis. The dipole moment of NPO is fully characterized by  $\mu_z$  only and it is directed from the  $\text{NO}_2$  group (−pole) toward the NO group (+pole). Methyl substitution in POM removes the rotational axis and the dipole moment lies in the molecular plane and its direction is affected greatly by the theoretical level. We computed the angles  $\alpha$  between the direction of the dipole vector and the line connecting the NO nitrogen and the C atom to which the  $\text{NO}_2$  group is attached (Table 1). It is found that  $\mu(\text{POM})$  still points toward the nitrone fragment but it is clearly rotated toward the methyl group by an angle  $\alpha \approx 45^\circ$  at the higher levels. The results obtained at the highest level are shown on top in Scheme 1. Also given in Table 1 are the projections of the dipole moments onto the line defined in said fashion and a line perpendicular to it. Remarkably, the RHF calculations

(32) Adeny, P. D.; Bouma, W. J.; Radom, L.; Rodwell, W. R. *J. Am. Chem. Soc.* **1980**, *102*, 4069.

(33) Boyd, S. L.; Boyd, R. J. *J. Phys. Chem.* **1994**, *98*, 11705.

(34) (a) With  $\text{CS}$  and  $\text{C}_2\text{H}_4$ : Sustmann, R.; Sicking, W.; Huisgen, R. *J. Am. Chem. Soc.* **1995**, *117*, 9679. (b) With  $\text{HNCO}$ : Matsuoka, T.; Harano, K. *Tetrahedron* **1995**, *23*, 6451.

(35) Christensen, D.; Jørgensen, K. A.; Hazell, R. G. *J. Chem. Soc., Perkin Trans. 1* **1990**, 2391.

(36) Electronic structures were explored via photoelectron spectroscopy: Houk, K. N.; Caramella, P.; Munchausen, L. L.; Chang, Y.-M.; Battaglia, A.; Sims, J.; Kaufman, D. C. *J. Electron Spectrosc. Relat. Phenom.* **1977**, *10*, 441.

(37) Böttcher, C. J. F. *Theory of Electric Polarization*, Volume I on *Dielectrics in Static Fields*, 2nd ed.; revised by van Belle, O. C., Bordewijk, P., Rip, A. Elsevier Scientific: New York, 1973; p 179.

(38) (a) Medyantseva, E. A.; Andreeva, I. M.; Minkin, V. I. *Zh. Org. Khim.* **1972**, *8*, 146. (b) Minkin, V. I.; Medyantseva, E. A.; Andreeva, I. M.; Gorshkova, G. V. *Zh. Org. Khim.* **1973**, *9*, 148. (c) Rodina, L. L.; Kuruts, I.; Korobitsyna, I. K. *Zh. Org. Khim.* **1981**, *17*, 1916.

(39) Jennings, W. B.; Boyd, D. R.; Waring, L. C. *J. Chem. Soc., Perkin Trans. 2* **1976**, 610.

(29) (a) RHF and MP2 theory employing a variety of basis sets: Irle, S.; Krygowski, T. M.; Niu, J. E.; Schwarz, W. H. E. *J. Org. Chem.* **1995**, *60*, 6744. (b) RHF/6-31G\*\* and RHF/6-311++G\*\* study: Gorse, D.; Cavagnat, D.; Pesquer, M.; Lapouge, C. *J. Phys. Chem.* **1993**, *97*, 4262. (c) MP2/6-31G\*: Lammertsma, K.; Prasad, B. V. *J. Am. Chem. Soc.* **1993**, *115*, 2348. (d) LDF theory: Habibollahzadeh, D.; Murray, J. S.; Grice, M. E.; Politzer, P. *Int. J. Quantum Chem.* **1993**, *45*, 15. (e) Comparisons to experiment are made, for example, in Table 2 in ref 29a and Table 1 in ref 29c. (f) CNDO theory suggested the *eclipsed* structure to be preferred: Prasad, P. L.; Singh, S. *Chem. Phys. Lett.* **1975**, *32*, 265. (g) Molecular Mechanics studies: Allinger, N. L.; Kuang, J.; Thomas, H. D. *J. Mol. Struct. (THEOCHEM)* **1990**, *209*, 125.

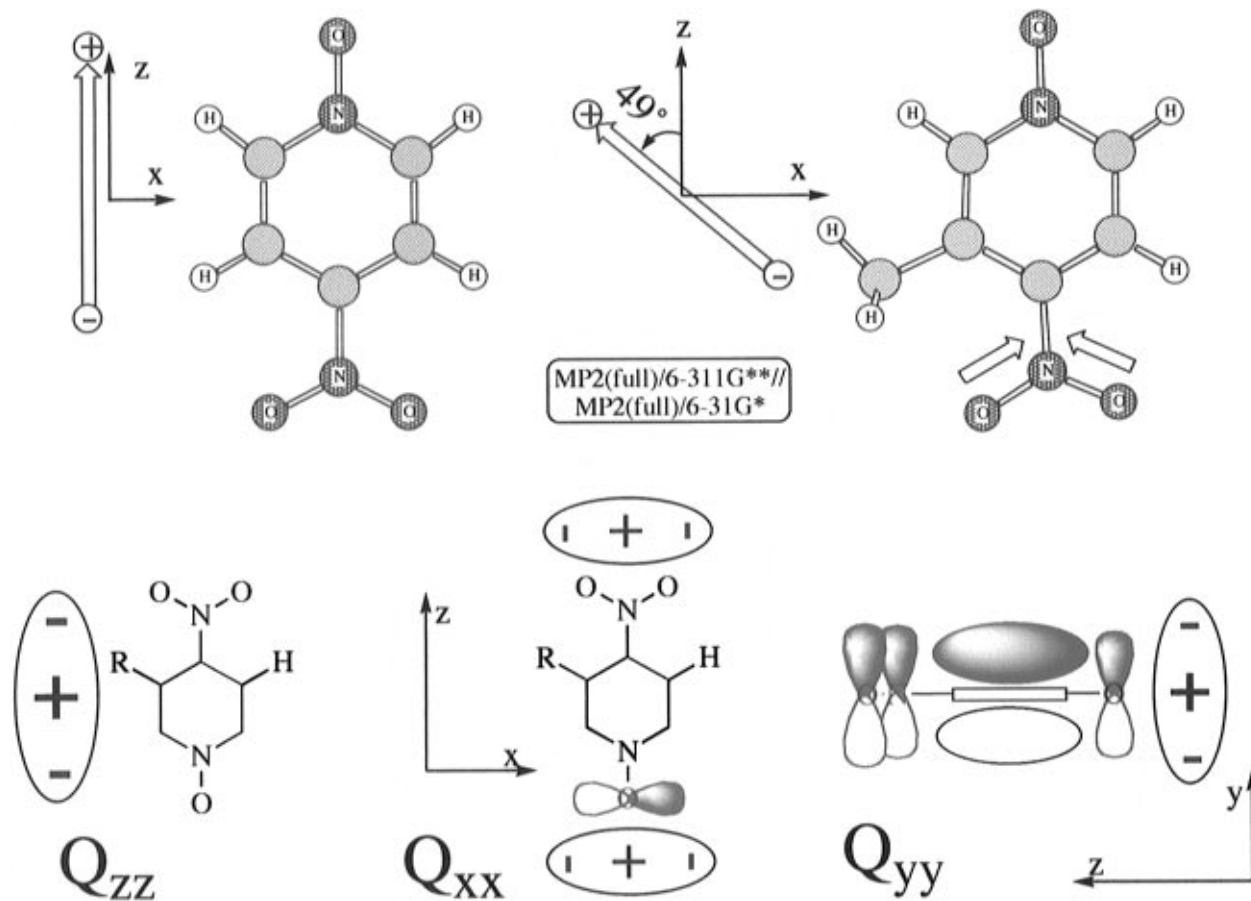
(30) (a) Tannenbaum, E.; Myers, R. J.; Gwinn, W. D. *J. Chem. Phys.* **1956**, *25*, 42. (b) Cox, A. P.; Waring, S. *J. Chem. Soc., Faraday Trans. 2* **1972**, *68*, 1060. (c) Note that the best microwave structure<sup>30b</sup> was determined on the basis of the *eclipsed* structure.

(31) Review: Tufariello, J. J. *Acc. Chem. Res.* **1979**, *12*, 396.

**Table 2. Dipole Moments of Nitromethane and *N*-Methylformaldimine *N*-Oxide<sup>a</sup>**

method	$\mu_x$	$\mu_y$	$ \mu $	$ \mu _{\text{NP}}$	$ \mu _{\text{MP}}$	$\mu_x$	$\mu_y$	$ \mu $	$ \mu _{\text{NP}}$	$ \mu _{\text{MP}}$
<i>ecl</i> -CH <sub>3</sub> NO <sub>2</sub>						<i>stag</i> -CH <sub>3</sub> NO <sub>2</sub>				
RHF/6-311G**	0.15	-4.08	4.08	5.15	5.09	-0.23	-4.07	4.08	5.15	5.09
MP2(full)/6-311G**	0.11	-3.35	3.36	4.40	4.19	-0.26	-3.34	3.35	4.40	4.19
Becke3LYP/6-311G**	0.09	-3.54	3.54	4.69	4.30	-0.19	-3.54	3.54	4.69	4.30
<i>anti</i> -H <sub>2</sub> C=N(O)CH <sub>3</sub>						<i>syn</i> -H <sub>2</sub> C=N(O)CH <sub>3</sub>				
RHF/6-311G**	-3.45	-2.98	4.55	6.09	5.37	3.72	-2.57	4.52	6.08	5.20
MP2(full)/6-311G**	-1.89	-2.88	3.45	4.84	4.16	2.17	-2.65	3.42	4.85	4.00
Becke3LYP/6-311G**	-2.32	-2.81	3.64	5.19	4.29	2.53	-2.55	3.59	5.17	4.09

<sup>a</sup> Dipole moment in debye. Nitromethane is oriented such that the C-N bond is aligned with the *y*-direction and the *xy*-plane is the symmetry plane for both conformations. The unique methyl H-atoms in the nitromethane structures are oriented in the positive *x*-direction. Abbreviations: NP = natural population, MP = Mulliken population.

**Scheme 1**

predict a dipole moment that is directed perpendicular to the *z*-axis.

As with the solution data,<sup>21</sup> our best estimates of  $\mu$ -(NPO) = 0.97 D and  $\mu$ -(POM) = 0.89 D show a small difference between the dipole moments with  $\mu$ -(NPO) being slightly larger than  $\mu$ -(POM), and both values are about 0.2 D higher than the values measured in solution. Note that the RHF dipole moments would seem to agree excellently both with the highest level computed data and the measured dipole moments, whereas the DFT data deviate the most. In light of the data provided in Table 2, it is clear that the agreement at the RHF level is fortuitous and due to cancellation of overestimated bond polarities. The same is true for the MNDO dipole moment. On the other hand, DFT theory does improve the description of the electron density distribution, but this may not necessarily result in the correct dipole moment.

**Quadrupole Moments of NPO and POM.** Calculated quadrupole moments of NPO and POM are summarized in Table 3. The elements  $Q_{ij}$  of the quadrupole moment tensor contain one term for the nuclear contribution and a second term to account for the contribution of the electron density distribution.<sup>40</sup> The values

$$Q_{ii} = \sum Z(n) R_i(n)^2 - \int \rho(\mathbf{r}) R_i^2 \quad i = x, y, z$$

$$Q_{ij} = 0.5 \sum Z(n) [3R_i(n) R_j(n) - \delta_{ij} R(n)^2] - 0.5 \int \rho(\mathbf{r}) [3R_i(n) R_j(n) - \delta_{ij} R(n)^2]$$

$Z(n)$  and  $R_i(n)$  refer to the nuclear charge and to the coordinates ( $i = x, y, z$ ) of atom  $n$ , and the sum runs

(40) For ab initio studies of the quadrupole moment of benzene, see: (a) Ha, T.-K. *Chem. Phys. Lett.* **1981**, 79, 313. (b) Dougherty, D. A. *Science* **1996**, 271, 163.

**Table 3. Quadrupole Moments of NPO and POM**

method	NPO			POM			
	$Q_{xx}$	$Q_{yy}$	$Q_{zz}$	$Q_{xx}$	$Q_{yy}$	$Q_{zz}$	$Q_{xz}$
RHF/6-311G**	-48.60	-56.58	-85.43	-53.68	-62.78	-92.41	1.25
MP2(full)/6-311G**	-50.04	-56.72	-78.38	-55.66	-63.02	-84.79	1.08
Becke3LYP/6-311G**	-49.38	-56.08	-79.85	-54.58	-62.31	-85.84	1.22

<sup>a</sup> The symmetry axis of NPO coincided with the  $z$ -axis and the molecule lies in the  $xz$ -plane. POM lies in the  $xz$ -plane as well and the  $z$ -axis coincides with the line connecting the NO nitrogen and the C atom to which the nitro group is attached. All values in D Å.

over all atoms. The off-diagonal elements  $Q_{ij}$  vanish whenever the molecule has a plane of symmetry perpendicular to either of the coordinates  $i$  or  $j$ , while the diagonal elements always have to be finite. The molecules NPO and POM lie in the  $xz$  plane and the functional groups are oriented along the  $z$ -axis. The  $C_{2v}$  symmetry of NPO causes all off-diagonal elements to vanish. The H/Me replacement destroys the rotational symmetry about the  $z$ -axis and  $Q_{xz}$  is nonzero, but it remains very small. The quadrupole moments of both NPO and POM are dominated by the diagonal elements, and all of these are negative. Negative  $Q_{ii}$  values indicate that, on average, the centers of negative charge are farther removed from the center of the molecule as compared to the position of the nuclei. Hence, in all three independent directions the molecules are characterized by the quadrupolarity  $\{- + -\}$ . As is indicated in the bottom row of Scheme 1,  $Q_{zz}$  characterizes the quadrupole due to the two electron-rich functional groups being connected to an electron deficient hydrocarbon core,  $Q_{xx}$  characterizes the  $(\delta^-)\text{O}-\text{N}(\delta^+)-\text{O}(\delta^-)$  polarity of the  $\text{NO}_2$  group and the lone-pair density at the nitron-O (with small contributions by the CH bonds), and  $Q_{yy}$  reflects the  $\pi$ -cloud typical for all aromatic systems. These values may be compared to  $p$ -nitroaniline (PNA), a typical and pertinent donor-acceptor type NLO material, for which values of  $Q_{xx} = -52.13$ ,  $Q_{yy} = -59.98$ , and  $Q_{zz} = -56.71$  D Å were calculated at the RHF/6-31G\* level for the  $C_{2v}$  structure in the same orientation as was used for NPO and POM. By way of comparison it becomes clear that  $Q_{xx}$  and  $Q_{yy}$  for the pyridine  $N$ -oxides are relatively "normal" and that  $Q_{zz}$  stands out. The  $Q_{zz}$  values of NPO and POM are some 30 D Å larger than for PNA and  $Q_{zz}(\text{POM})$  is clearly larger than  $Q_{zz}(\text{NPO})$ .

**Point Charge Models of NPO and POM.** The concept of "atomic charge" is central to discussions of the properties and reactivity of molecules, and many methods have been proposed to assign charges to atoms. Basis set partitioning and density partitioning methods have been developed.<sup>41</sup> To the class of basis set partitioning methods belong, for example, the historically significant Mulliken population (MP) analysis<sup>42</sup> and its more modern variations,<sup>43</sup> as well as the natural population (NP) analysis.<sup>44</sup> The NP analysis is known to produce atomic charges that are in close agreement with charges derived from topological electron density analysis.<sup>45a</sup> The Mulliken partitioning scheme splits the

**Table 4. Natural Population Analyses of NPO and POM<sup>a</sup>**

atom	NPO				POM			
	RHF	MP2	DFT	$\kappa$	RHF	MP2	DFT	$\kappa$
N1(O)	0.14	0.10	0.10	0.09	0.15	0.10	0.10	0.22
C2	0.03	0.00	0.00	-0.18	0.01	0.00	-0.01	-0.13
C2H	0.25	0.22	0.23	0.07	0.23	0.22	0.22	0.06
C3	-0.15	-0.21	-0.19	-0.09	0.04	-0.02	0.00	0.00
C4	0.03	0.05	0.04	-0.16	0.01	0.05	0.04	-0.11
C5	-0.15	-0.21	-0.19	-0.16	-0.14	-0.21	-0.18	-0.04
C5H	0.09	0.04	0.06	0.00	0.10	0.04	0.07	0.10
C6	0.03	0.00	0.00	-0.06	0.01	0.00	-0.01	0.05
C6H	0.25	0.22	0.23	0.03	0.23	0.22	0.22	0.18
O7	-0.59	-0.44	-0.46	-0.14	-0.59	-0.44	-0.46	-0.44
N8	0.65	0.45	0.50	0.42	0.65	0.45	0.50	0.48
O9	-0.45	-0.34	-0.38	-0.14	-0.46	-0.35	-0.39	-0.40
O10	-0.45	-0.34	-0.38	-0.14	-0.45	-0.35	-0.39	-0.40
Me/H11	0.24	0.25	0.25	0.05	0.09	0.08	0.09	0.29
$\Sigma(\text{NO})$	-0.45	-0.33	-0.36	-0.05	-0.44	-0.34	-0.36	-0.22
$\Sigma(\text{C}_5\text{H}_3\text{R})$	0.71	0.57	0.62	-0.10	0.70	0.58	0.63	0.52
$\Sigma(\text{NO}_2)$	-0.25	-0.23	-0.27	0.14	-0.26	-0.24	-0.28	-0.32

<sup>a</sup> All calculations employed the 6-311G\*\* basis set. MP2 indicates MP2(full). DFT indicates Becke3LYP. See introduction for numbering scheme. The entries C%H specify the group charge of C% together with the attached H atom. Populations from  $\kappa$  refinement taken from ref 16 (NPO) and ref 17 (POM).

overlap population equally between the bonded atoms, and this causes grave errors in polar systems. The NP analysis is advantageous in systems with bonds of high polarity, and the results of the NP analysis for NPO and POM are summarized in Table 4.

The variations among the atom and fragment charges depending on the theoretical levels follow expected patterns. RHF bond polarities are overestimated, and the perturbational treatment counteracts. The hybrid method intrinsically generates data that are within the interval defined by the RHF and MP2 methods, and they are generally closer to the MP2 data.<sup>46</sup> We will focus on the best data obtained at the MP2(full)/6-311G\*\*//MP2(full)/6-31G\* level. The NP charges determined for the NO and  $\text{NO}_2$  functional groups and for the hydrocarbon midsection indicate a highly quadrupolar molecule in which more than one-half of an electron was removed from the midsection. Moreover, they indicate that more of the negative charge is accumulated on the NO group than on the  $\text{NO}_2$  group. The electron density distribution revealed by the NP analysis provides a significantly different picture as compared to the one expected based on simple qualitative valence bond considerations. Considering possible

(41) Glaser, R. *J. Comput. Chem.* **1989**, 10, 118.

(42) Mulliken, R. S. *J. Chem. Phys.* **1955**, 23, 1833.

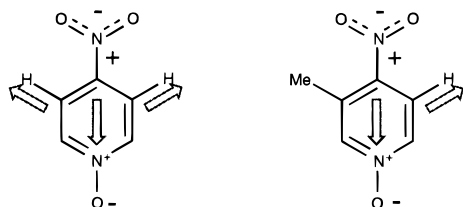
(43) (a) Huzinaga, S.; Narita, S. *Isr. J. Chem. Phys.* **1980**, 19, 242. (b) Huzinaga, S.; Sakai, Y.; Miyoshi, E.; Narita, S. *J. Chem. Phys.* **1990**, 93, 3319.

(44) (a) Reed, A. E.; Weinstock, R. B.; Weinhold, F. *J. Chem. Phys.* **1985**, 83, 735. (b) Carpenter, J. E.; Weinhold, F. *J. Mol. Struct. (THEOCHEM)* **1988**, 169, 41. (c) Arnaud, R. *J. Comput. Chem.* **1994**, 15, 1341 and references therein.

(45) (a) Bader, R. F. W. *Atoms in Molecules—A Quantum Theory*; Clarendon Press: Oxford, UK, 1990. (b) Slee, T. *J. Am. Chem. Soc.* **1986**, 108, 7541. (c) Bader, R. F. W.; Larouche, A.; Gatti, C.; Carroll, M. T.; MacDougall, P. J.; Wiberg, K. B. *J. Chem. Phys.* **1987**, 87, 1142. (d) Glaser, R.; Choy, G. S.-C. *J. Am. Chem. Soc.* **1993**, 115, 2340. (e) Glaser, R. *J. Comput. Chem.* **1990**, 11, 663.

(46) We also analyzed the respective data obtained with the 6-31G\* basis set and obtained virtually the same numbers. Basis set dependencies are small in the NP analysis, and this will also come to the fore in the discussion of the point charge model derived approximate dipole moments.

contributions by the quinoid resonance form **II** (vide supra), one might expect the dipole vectors of NPO and POM to point from a negatively charged NO<sub>2</sub> group to a positively charged NO group. The dipole direction is indeed realized but for an entirely different reason! The resonance form **II** does not contribute significantly to the electronic ground states of NPO and POM and their dipole directions are not caused by electron density shifts from the NO to the NO<sub>2</sub> group. The electronic structures of the pyridine *N*-oxides are just what one would predict based on atom electronegativities. The positive end of the molecular dipole moment of each pyridine *N*-oxide is pointed toward the area of highest electron accumulation (the NO group)<sup>47</sup> as the simple result of the vector addition of the two inward-pointing dipoles that are associated with the functional groups. The basic electronic motif is common to NPO and POM, and it is clearly manifested at all of the theoretical levels. At each theoretical level, the variations between NPO and POM are marginal (<0.02) with the *only* exception concerning the C3 atom and the attached group (H or Me) since methyl substitution replaces the weakly polar ( $\delta^-$ )C3–H( $\delta^+$ ) bond with the even less polar C–C bond:



Hence, the bond dipole moment associated with the C5–H bond is unopposed in POM, and this fact should contribute to a rotation of the molecular dipole moment in the opposite direction as is actually observed. Hence, the  $\alpha$  angle must have another origin. One possible explanation lies with the structural distortions due to steric interactions between the nitro and the methyl groups which cause the  $\angle$ (C3–C4–N8) angle to widen. This distortion causes a rotation of the dipole moment component associated with the N–O bonds (as indicated in Scheme 1) in the direction indicated by the  $\alpha$  angle for the molecular dipole moment.

The theoretically determined charges may be compared to the populations determined via  $\kappa$  refinement of the solid-state electron density and the respective data for NPO<sup>16</sup> and POM<sup>17</sup> (Table 4). A drastic difference comes immediately to the fore: While atomic charges are hardly affected by the 3-methyl substitution in the theoretical analysis, major differences occur between the populations *P* of NPO and POM. The *P* data set for POM agrees better with the NP data, and both methods reflect the quadrupolar motif due to the functional groups and the hydrocarbon core but the NPO data completely fail to do so. The NPO *P* data deviate generally more, and they even indicate a positive charge on the NO<sub>2</sub> group which is inconsistent with fundamental ideas about ionization potentials and electronegativity. While the electron density analysis of NPO by Coppens et al.<sup>16</sup> was an early and pioneering

**Table 5. Molecular and Point Charge Model Derived Dipole Moments for NPO and POM<sup>a</sup>**

method	$\alpha$ (deg)	$ \mu $	$ \mu _{\text{NP}}^b$	$ \mu _{\text{MP}}^b$
NPO				
RHF/6-311G**		0.24	0.25	1.77
MP2(full)/6-311G**		0.97	1.11	2.18
Becke3LYP/6-311G**		1.25	1.44	2.37
POM				
RHF/6-311G**	96.1	0.87	84.4	0.81
MP2(full)/6-311G**	48.7	0.89	36.3	1.08
Becke3LYP/6-311G**	43.2	1.21	34.0	1.49

<sup>a</sup> Dipole moments in debye. <sup>b</sup> Values  $|\mu|$  are the directly computed molecular dipole moments, while the approximate dipole moments  $|\mu|_{\text{NP}}$  and  $|\mu|_{\text{MP}}$  are derived from point charge models as described in the text.

contribution to high-resolution X-ray analysis, refinement methods have evolved in the past two decades, and it will be of interest to see whether the more sophisticated aspherical atom refinement methods<sup>48</sup> will resolve this discrepancy. This analysis of the *P* data reveals an apparently paradox situation in which the population data that better reflect the polar nature of POM result in a point charge model (PCM) derived dipole moment that is greatly in error and vice versa for NPO. The paradox is resolved with the realization that a partitioning scheme is not validated by its ability to reproduce the molecular dipole moment. Huzinaga pointed out that an accurate reproduction of the molecular dipole moment requires a point charge model with off-center terms as well.<sup>43</sup> Alternatively, it is possible to reproduce the molecular dipole by supplementing the point charge model with additional point dipole moments located at the positions of the nuclei. The latter approach has been implemented within Bader's theory of atoms in molecules.<sup>45</sup>

The point charges determined with the natural population (NP) and the Mulliken population (MP) analysis schemes were employed to compute the approximate dipole moments  $\mu_{\text{NP}}$  and  $\mu_{\text{MP}}$ , respectively. These values are calculated using the equation  $\mu = \sum_i (q_i \mathbf{r}_i)$  where the summation is over all *i* atoms of the molecule. The vectors  $\mathbf{r}_i$  refer to the locations of the atoms, and  $q_i$  are the atomic charges determined with one of the partitioning methods. Numerical results obtained for the PCM-derived dipole moments at six theoretical levels are given in Table 5 for NPO and POM and in Table 2 for the nitro and nitron models. The PCM dipoles of the model systems consistently show an overestimation of the polarity by 25–50%, and this is true for both the  $|\mu|_{\text{NP}}$  and  $|\mu|_{\text{MP}}$  values. The seemingly good agreement between the molecular dipoles and the  $|\mu|_{\text{NP}}$  values of NPO (within 0.2 D) and POM (within 0.4 D) must be considered as fortuitous and can be traced to partial cancellation of two overestimated components. Neither  $\mu_{\text{NP}}$  nor  $\mu_{\text{MP}}$  can provide a good estimate of the molecular dipole moment.

## Conclusion

The dipole moments of NPO and POM were examined using correlated levels of ab initio theory in conjunction with valence triple- $\zeta$  quality, and fully polarized basis sets and dipole moments of  $\mu(\text{NPO}) = 0.97$  and  $\mu(\text{POM})$

(47) For violations of the approximate relation  $\mu \propto \chi(A) - \chi(B)$ , see: Huzinaga, S.; Miyoshi, E.; Sekiya, M. *J. Comput. Chem.* **1993**, *14*, 1440.

(48) Wood, J. S. *Inorg. Chim. Acta* **1995**, *229*, 407 and references therein.

= 0.89 D were obtained. At this level of theory, the agreement between experiment and theory is quite good, and, as with the solution data, the gas-phase dipole moments show a small reduction in dipole moment upon methyl substitution. We conclude that methyl substitution affects the dipole moment only very slightly and leads to a small reduction of  $0.14 \pm 0.10$  D.

The quadrupole moments of NPO and POM are dominated by the diagonal elements and all of these are negative and indicate quadrupolarity  $\{- + -\}$  along all axes. The  $Q_{zz}$  values of NPO and POM are particularly large in absolute value—as is typical for a quadrupolar molecule with a small dipole moment—and  $|Q_{zz}(\text{POM})| = 85 \text{ D \AA}$  is significantly larger than  $|Q_{zz}(\text{NPO})| = 78 \text{ D \AA}$ . Natural population analysis indicates that the electronic consequences of H/Me replacement are localized. This basic electronic motif—electron-rich NO and NO<sub>2</sub> groups and electron-deficient hydrocarbon mid-section—is common to NPO and POM. The theoretical results show that the dipole moment is pointed from the NO<sub>2</sub> group (−pole) toward the NO group (+pole) although the NO group is the area of highest electron accumulation in the pyridine *N*-oxides. The dipole moment in POM is rotated such as to point toward the Me-substituted half, and this rotation likely is due to steric repulsion between the methyl and nitro groups. The population analysis points out that the dipole directions in pyridine *N*-oxides *do not* reflect contributions by the quinoid resonance form. Instead, the dipoles result from vector addition of the inward-pointing dipoles associated with the functional groups. The molecular dipoles are governed by electronegativity differences between bonded atoms and not by conjugation effects.

The “molecular dipole moments” determined for NPO and POM based on the solid state are point charge model (PCM) derived quantities. Our discussion shows that PCM-derived dipoles of dipolar species are overestimated and therefore provide an upper limit value. For quadrupolar systems with near-zero dipoles one can hope for some cancellation of errors, but it is clear that a large uncertainty remains. Since the dipole moments of the opposing functional groups are about 4 D and the PCM derived dipoles may deviate from these by 25–50%, one can hope at best for an accuracy of 1 D (25% of component) for the PCM-derived dipole moment. In light of these possible errors, a discussion of solid-state effects on the molecular dipole moments of NPO and POM must be postponed until the true molecular dipole moments in the crystal have been more rigorously established.

**Acknowledgment** is made to the MU Research Board for support of this research. We thank the MU Campus Computing Center for generous allocations of resources. Part of this research was conducted using the resources of the Cornell Theory Center, which receives major funding from the National Science Foundation and the New York State with additional support from the Advanced Research Projects Agency, the National Center for Research Resources at the National Institutes of Health, IBM Corp., and the members of the Corporate Research Institute.

**Supporting Information Available:** Total energies and properties determined with the 6-31G\* basis set (6 pages). See any current masthead page for ordering and Internet access instructions.

CM960433U